Time-dependent energetic proton acceleration and scaling laws in ultraintense laser-pulse interactions with thin foils

Yongsheng Huang (黄永盛),[1,2,*] Yuanjie Bi (毕远杰),[1,2] Yijin Shi (施义晋),[1] Naiyan Wang (王乃彦),[1] Xiuzhang Tang (汤秀章),[1] and Zhe Gao[2]

[1]*China Institute of Atomic Energy, Beijing 102413, China*

[2]*Department of Engineering Physics, Tsinghua University, Beijing 100084, China*

(Received 9 October 2008; revised manuscript received 15 January 2009; published 25 March 2009)

A two-phase model, where the plasma expansion is an isothermal one when laser irradiates and a following adiabatic one after laser ends, has been proposed to predict the maximum energy of the proton beams induced in the ultraintense laser-foil interactions. The hot-electron recirculation in the ultraintense laser-solid interactions has been accounted in and described by the time-dependent hot-electron density continuously in this model. The dilution effect of electron density as electrons recirculate and spread laterally has been considered. With our model, the scaling laws of maximum ion energy have been achieved and the dependence of the scaling coefficients on laser intensity, pulse duration, and target thickness have been obtained. Some interesting results have been predicted: the adiabatic expansion is an important process of the ion acceleration and cannot be neglected; the whole acceleration time is about 10–20 times of laser-pulse duration; the larger the laser intensity, the more sensitive the maximum ion energy to the change of focus radius, and so on.

DOI: 10.1103/PhysRevE.79.036406 PACS number(s): 52.38.Kd, 41.75.Jv, 52.40.Kh, 52.65.−y

I. INTRODUCTION

Proton acceleration mechanisms in ultraintense laser pulses interaction with thin solid targets attract more and more interest nowadays [1]. Various models [2–5] have been presented to estimate the maximum energy of proton beams. However, the models given by Wilks *et al.* [1], Kaluza *et al.* [2], Schreiber *et al.* [3], and Fuchs *et al.* [4] are all based on isothermal expansions of quasineutral plasmas [6]. Robson *et al.* [5] presented a two-phase temperature-varying model, where the hot-electron temperature first increases linearly on the pulse duration timescale and then decreases adiabatically with time. However, in the pulse duration, does the hot-electron temperature rise up linearly? That is still difficult to validate. Generally one assume that when an ultraintense laser pulse interacts with a solid target, the laser-produced fast electrons with a uniform temperature, k_BT_e, determined by the laser ponderomotive potential are instantly created in front of the target, propagate through the target collisionlessly, and then form a high energy plasma at the rear of the target. When the laser pulse still exists, the hot-electron temperature, $k_BT_e=m_ec^2(\gamma-1)$, is assumed invariant due to a constant energy supply from the laser pulse, where $\gamma=(1+I\lambda^2/1.37)^{0.5}$ is the relativistic factor, I is the laser intensity in 10^{18} W/cm^2, λ is the laser wavelength in micrometers, m_e is the electron mass, and t_l is the pulse duration. The plasma expansion is an isothermal expansion. Therefore, a two-phase model different from Robson *et al.* [5] is proposed in this article, where the plasma expansion is isothermal in the laser-pulse duration and then the hot-electron temperature decreases as $(t/t_l)^{-(1+1/\gamma)}$ [7].

The electron-density distribution satisfies Boltzmann relationship $n_e=n_{e0}\exp(e\phi/k_BT_e)$ and n_{e0} stays constant and time-independent in the previous models [2–4,6] without hot-electron recirculation, where e is the elementary charge and ϕ is the electric potential. Therefore, with a little adjustment of some parameters, the acceleration time [3,4], the opening angle of electrons [2], and electron density, n_{e0} [2–4], Mora's result can be used to estimate the maximum energy of proton beams for thick targets, where the influence of hot-electron recirculation on the ion acceleration can be ignored. Although Robson *et al.* [5] have presented a two-phase model which is consistent with experiments, the hot-electron recirculation is still ignored. However, Mackinnon *et al.* [8] observed enhancement of proton acceleration by hot-electron recirculation in thin foils whose thickness is less than a critical value. In addition, Sentoku *et al.* [9] predicted an equation to conclude the influence of electron recirculation and proved that the hot-electron recirculation cannot be ignored in the laser-foil interactions, although they did not propose a clear description of electron recirculation and their physical picture is too simple and not clear. The assumption that the maximum hot-electron density for a thin foil is a constant and N times of the value for a critical target thickness in the model of Sentoku *et al.* [9] is rough and unreasonable. Because there are n times of the electron recirculation, they happen one after the other and the electron density cannot jump to n times of the initial density. After that, Huang *et al.* [10] presented a step model to describe the influence of the hot-electron recirculation on the laser-ion acceleration. In the step model, the hot-electron density rises step by step with isothermal plasma expansions. In fact, the electron density should rise continuously and then decrease to zero as the time tends to infinite. Therefore, the time-dependent hot-electron density and the electric field are necessary for the description of the hot-electron recirculation and the whole process of the ion acceleration. The dilution effect of the electron density as the electrons circulate and spread laterally should be considered but not accounted in the previous models [9,10].

In Sec. II, a two-phase model which contains three-dimensional effect (the thickness effect and the angular ef-

*hyc05@mails.tsinghua.edu.cn

TABLE I. This is a comparison between our two-phase model and some experiments for $\theta_{in}=30°$ in Ref. [2], $\theta_{in}=22°$ in Ref. [8], and $\theta_e=17°$ in Ref. [13].

I (10^{18} W/cm^2)	λ (μm)	t_l (fs)	r_L (μm)	L (μm)	$\eta(L)$ (%)	$n_{e0}(L)$ (10^{20}/cm^3)	E_{max} from experiments or PIC (MeV)	E_{max} from our model (MeV)
10	0.79	150	2.5	30	40	0.33	1.2 ± 0.3 [a]	1.1
10	0.79	150	2.5	20	40	0.81	2.0 ± 0.3 [a]	2.0
13	0.79	150	2.5	30	40	0.36	1.5 ± 0.3 [a]	1.4
15	0.79	150	2.5	30	40	0.37	1.7 ± 0.3 [a]	1.6
100	0.8	100	2.5	3	40	14.2	22–24[b]	22.6
100	0.8	100	2.5	6	40	8.6	17–19[b]	17.3
100	0.8	100	2.5	10	40	5.13	11–17[b]	13.2
100	0.8	100	2.5	25	40	0.897	6–7[b]	5.0

[a]Reference [2].
[b]Reference [8].

fect, which are discussed in detail by Huang *et al.* [10], and the dilution effect as the electrons circulate and spread laterally) and hot-electron recirculation is proposed, where the plasma expansion is isothermal in the pulse duration and then adiabatic. The main processes of our model are two: first, combining the Mora's result in Ref. [6] and the increase of the electron density in the pulse duration, with the assumption that the hot-electron temperature is a constant and the dependence hot-electron density, the electric field, and the ion velocity on the time are obtained; second, with the assumption of an adiabatic expansion, the dependence of the temperature of hot electrons on time as proposed by Mora [7] has been used and then the maximum ion velocity is obtained easily. A most significant progress of our model is that the time-dependent electric field and hot-electron density can be given easily by solving two nonlinear equations. As a result of the model, the duration of the time-dependent electric field at the ion front is approximately 1–2 times of the main laser-pulse duration which is consistent with the result presented by d'Humières *et al.* [11] using the particle-in-cell (PIC) simulation. The whole acceleration time is about 10–20 times of the laser-pulse duration. Moreover, we also proofed that the adiabatic expansion is an important process for the ion acceleration and cannot be neglected. Our model can be used in the same application content as the model of Robson *et al.* [5]. However, from the above discussions, our model is more reasonable and easier to use than theirs.

In Sec. III, in the ultrahigh-contrast region, the comparison between our time-dependent model, the step model [10], and the experiments of Saclay [12] has been shown in Fig. 2. With a proper laser absorption efficiency for thick targets, our two-phase model has also been compared to other experiments and they are consistent as shown in Table I. The laser absorption stays constant with the target thickness for thick target. The laser absorption efficiency for the target of arbitrary thickness has been calculated by PIC simulations [11], although there is no analytic result of that. With the laser absorption efficiency of 40% for the target of 3 μm given by the result of PIC simulations, the comparison between our model and the experimental result is shown in Table I. If the laser absorption is known, for the target of arbitrary thickness, the maximum energy of proton beams and time-dependent electric field and electron density can all be obtained using our model.

In Sec. IV, with our two-phase model, the scaling law of maximum ion energy with respect to laser intensity for a series of constant pulse duration has been given and discussed as shown in Fig. 3. The dependence of maximum ion energy on target thickness, focus radius, and laser-pulse duration has been obtained. With the scaling law, some interesting results have been obtained and discussed in detail. In Sec. II, the limits of our model have been discussed.

II. TIME-DEPENDENT ENERGY PROTON ACCELERATION

For convenience, the physical parameters, time t, ion position l, ion velocity v, electron field E, hot-electron density n, and light speed c, are normalized as Eq. (1) in [10]. Then the normalized parameters are τ, $\hat{l}$, u, $\hat{E}$, $\hat{n}$, and $\hat{c}$ as shown by Eq. (1) in [10].

When an ultraintense laser pulse interacts with a solid target, the laser-produced fast electrons with a uniform temperature, k_BT_e, determined by the laser ponderomotive potential are instantly created in front of the target and propagate through the target and then form a high energy plasma at the rear of the target. Here, it is assumed that the hot-electron transport is free, which is true for high energetic electrons, thin foils, or when the atomic number of the materials of the target is low. Hot electrons at the rear of the target can be considered to be reflected by sheath field at the ion front [13] and come back to the front of the target because the field there is strongest. Once hot electrons are created, they will bounce between the ion front before the target and the ion front at the rear side. Since we consider that the electron motion is collisionless, the bounce of hot electrons will last in the whole time of the plasma expansion. When the hot electrons propagate through the target, the electron beam can be assumed to be in equilibrium.

A. Isothermal expansion

The hot-electron speed used is the light speed c. Here the choice of $t=0$ is the same as that in the step model given by

Huang *et al.* [10]. For simplicity in the $-L/c \le t \le t_l - L/c$, where L is the target thickness, the laser intensity is assumed to be a constant, therefore, the hot-electron temperature, $k_B T_e = m_e c^2(\gamma - 1)$, is invariant. The plasma expansion is an isothermal expansion.

The fast-electron density is a function of the parameters acceleration time τ, the target thickness L, laser intensity I, laser focus radius r_L, laser absorption efficiency η, the incidence angle of the laser pulse θ_{in}, and the half-opening angle of fast electrons θ_e. The time-dependent electron density is assumed

$$n_e(\tau, L, I, r_L, \eta, \theta_{\text{in}}, \theta_e) = N(\tau, L) n_{e0}(L, I, r_L, \eta, \theta_{\text{in}}, \theta_e),$$

$$N(\tau, L) = 1, \tau = \tau_1 = \tau_L, \tag{1}$$

where τ_1 is the time when the zeroth hot-electron recirculation ends and hot electrons go forth to reach the rear of the target the second time, $\tau_L = 2\hat{L}/c/\sqrt{2e}$; here e denotes the numerical constant 2.718 28… . $n_{e0}(L, I, r_L, \eta, \theta_{\text{in}}, \theta_e)$ is the hot-electron density when hot electrons return back from the ion front before the target and go forth to reach the rear of the target the second time, and $N(\tau, L)$ describes the increase of the maximum electron density due to electron recirculation and the electron generation by the laser-plasma interactions at the front of the target.

Using Eq. (2) in [2], since the total number of hot electrons that propagate through the target at $t = t_L = 2L/c$, $N_e = \eta(L) E_l / (k_B T_e)$ for $t_l \le t_L$ and $N_e = \eta(L) E_l t_L / (k_B T_e t_l)$ for $t_l \ge t_L$, n_{e0} in Eq. (1) can be estimated by

$$n_{e0} = \frac{4.077\,\eta(L) I_{10^{18}\ \text{W/cm}^2}}{(\gamma - 1)[1 + (L^*/r_L)\tan(\theta_e)]^2}, \quad t_l \ge t_L, \tag{2}$$

$$n_{e0} = \frac{4.077\,\eta(L) I_{10^{18}\ \text{W/cm}^2} t_l}{(\gamma - 1)[1 + (L^*/r_L)\tan(\theta_e)]^2 t_L}, \quad t_l \le t_L, \tag{3}$$

where r_L is the laser-pulse focus radius, $L^* = L/\cos(\theta_{\text{in}})$ is the efficient target thickness, θ_{in} is the incidence angle of the laser pulse, and $\theta_e \approx 17°$ is half-opening angle of the suprathermal electrons which was measured by Santos *et al.* [13]. With Eqs. (2) and (3), the three-dimensional effect has been accounted in through the considering of the half-opening angle of electrons, $\theta_e \approx 17°$. Note that the right side of Eq. (3) has a factor t_l/t_L, which is not in the right side of Eq. (2). For $t_l \le t_L$, $N_e = \eta(L) E_l / (k_B T_e)$, where E_l is the energy of laser pulse. However, for $t_l \ge t_L$, at $t = t_L$, hot electrons are still being generated by the laser-plasma interactions at the front of the target and the number of hot electrons which propagate through the target is a part of the total number, $N_e = \eta(L) E_l t_L / (k_B T_e t_l)$. Therefore, Eqs. (2) and (3) are obtained. When $r_L \gg L$ and $\tan(\theta_{\text{in}}) \ll 1$, $[1 + (L^*/r_L)\tan(\theta_{\text{in}})]^2 \approx 1$, the angular effect can be neglected. Therefore, the influence of $\eta(\hat{L})$ and electron recirculation become dominated for thin targets. For example, for $I = 3 \times 10^{20}$ W/cm^2, $\lambda = 1.053$ nm, and $t_l = 500$ fs [14], the temperature of hot electrons is about 5.5 MeV. For $\eta(L) = 50\%$, $r_L = 5$ μm, with Eq. (3), the electron density is about 4.8×10^{19} cm^{-3} and it is about the value measured by x ray in [14]. Since the laser-pulse duration is t_l, with similar discussion in [10], the critical target thickness for the hot-electron recirculation is $L_c = 0.5 c t_l$.

With reference to the discussion and method given by Huang *et al.* [10], the relationship between the ion velocity at the ion front and the electron density can be described by Eq. (12) in [10]. With that equation, the ion velocity is decided by $N(\tau)$. Therefore, the solution of $N(\tau)$ is a key point. Although it has been given by Huang *et al.* [10] with a simple model, it is rough for three reasons:

(1) it is discrete, however the actual electron density changes continuously;

(2) the electron density decreases as electrons recirculate and spread laterally and this dilute effect was not counted in the step model [10];

(3) the turning point of hot electrons at front of the target is not static but moving with the expansion of the plasma too.

Here, a more actual and valuable method will be proposed to calculate a continuous solution of $N(\tau)$ as follows.

Assuming that the velocity at the ion front before the target is the same as that at the rear of the target and the two turning points for the electron recirculation are the ion front before the target and at the rear, respectively, if hot electrons satisfy uniform distribution in the bulk from the ion front before the target to the ion front at the rear, $N(\tau)$ is decided by

$$N(\tau) = \frac{\int_{-\hat{L}/\hat{c}}^{\tau - \hat{L}/\hat{c}} f d\tau}{\int_{-\hat{L}/\hat{c}}^{\tau_L - \hat{L}/\hat{c}} f d\tau} \frac{\hat{L} + 2\hat{l}(\tau_L)}{2\hat{l}(\tau) + \hat{L}} F_{\theta,3\text{D}}, \quad \tau \le \tau_l, \tag{4}$$

where f represents the generation rate of hot electrons in the interaction of laser pulses with the plasma at the front of the target, $F_{\theta,3\text{D}} = \{\frac{f_\theta[\hat{L} + 2\hat{l}(\tau_L)] + \hat{r}_L}{f_\theta[\hat{L} + 2\hat{l}(\tau)] + \hat{r}_L}\}^2$ and $f_\theta = \tan(\theta)/\cos(\theta_{\text{in}})$. f depends on the absorption mechanisms of laser pulses and decides the density of hot electrons. The factor, $F_{\theta,3\text{D}}$, corresponds to the decrease of on-axis density as hot electrons circulate and spread laterally with a given opening angle, θ_e, and also it reflects three-dimensional effect on the ion acceleration. The special integrating limits are because there is an interval before the electrons generated by the laser pulse at the front of the target come to the rear. With the assumption $f = \bar{f}$ for $\tau \in [0, \tau_l]$, Eq. (4) can be simplified to be

$$N(\tau) = \frac{\tau}{\tau_L} \frac{\hat{L} + 2\hat{l}(\tau_L)}{2\hat{l}(\tau) + \hat{L}} F_{\theta,3\text{D}}, \quad \tau \le \tau_l, \tag{5}$$

B. Adiabatic expansion

When $t \ge t_l$, the laser pulse has gone and the acceleration field at the ion front decreases quickly for two reasons. First, the temperature of hot electrons decreases with time as shown by [7]

$$T_e \propto (\tau/\tau_l)^{-(1+1/\gamma)}, \tag{6}$$

where γ is the relativistic factor. In the nonrelativistic case, $\gamma = 1$, with Eq. (6), $T_e \propto t^{-2}$ which is consistent with all the

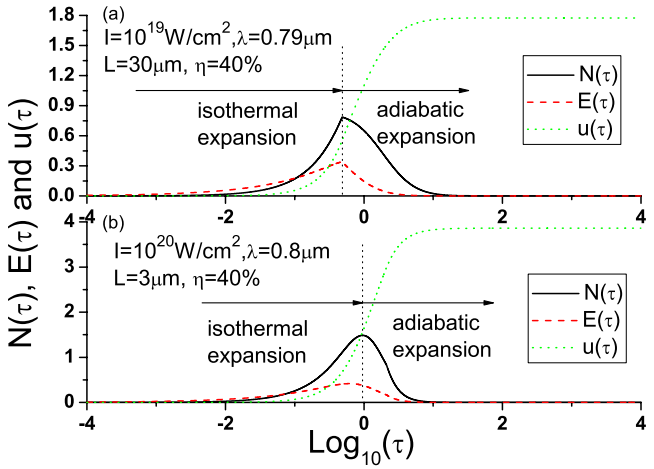

FIG. 1. (Color online) The time-dependent hot-electron density, acceleration field, and the speed of ions versus $\tau=\omega_{pi}t/\sqrt{2e}$ given by the time-dependent target normal sheath acceleration for $\theta_{\text{in}}=30°$ [in (a)], $\theta_{\text{in}}=22°$ [in (b)], $\theta_e=17°$, and $\eta=40\%$. In (a), the laser-pulse parameters are $I=1.0\times10^{19}$ W/cm^2, $\lambda=790$ nm, $r_L=2.5$ μm, $L=30$ μm, and $t_l=150$ fs. In (b), the laser-pulse parameters are $I=1.0\times10^{20}$ W/cm^2, $\lambda=800$ nm, $r_L=2.5$ μm, $L=3$ μm, and $t_l=100$ fs.

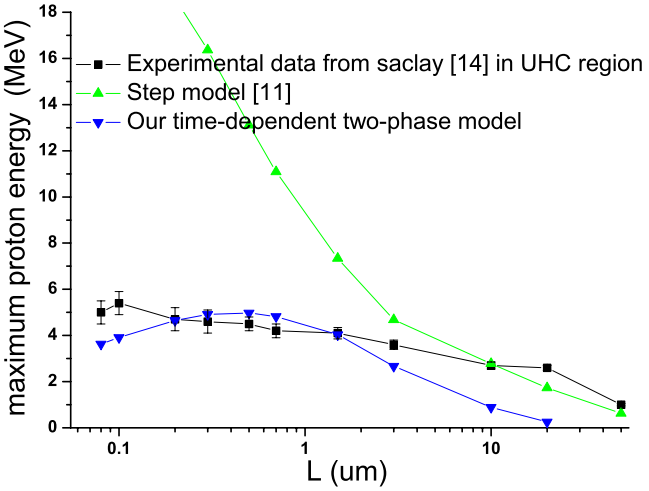

FIG. 2. (Color online) Maximum ion energy vs target thickness for $I=5\times10^{18}$ W/cm^2, pulse duration $t_l=65$ fs, $\lambda=800$ nm, and $r_L=4$ μm. For $L<L_c$, the results of our model are well consistent with the experimental data.

previous work of adiabatic expansion into a vacuum [15]. For the ultrarelativistic case, $\gamma\to+\infty$, with Eq. (6), $T_e\propto t^{-1}$ which is the same with Mora's results [7]. After the laser pulse vanishes, the ion front does not stop and the electron bulk still increases. Therefore, the electron density, $N(\tau)$, decreases as given by

$$N(\tau)=\frac{\tau_l}{\tau_L}\frac{\hat{L}+2\hat{l}(\tau_L)}{2\hat{l}(\tau)+\hat{L}}F_{\theta,3\text{D}},\quad \tau\geq\tau_l. \tag{7}$$

Equations (5) and (7) are all nonlinear differential equations and have no analytic solutions. However, the numerical results can be obtained by computer with iterative method. The initial $N(\tau)$ is given by the solution of the Eqs. (5) and (7) in which $F_{\theta,3\text{D}}\equiv1$. As an example, the solutions of a thin foil and a thick solid target have been given by Fig. 1. Figure 1(a) corresponds a thick target of 30 μm and the hot-electron recirculation can be ignored. Figure 1(b) corresponds a thin foil of 3 μm and the maximum value of $N(\tau)$ is about 1.5, which is lower than that given by Huang *et al.* [10] and Sentoku *et al.* [9] and reflects the three-dimensional effect. From Fig. 1, some interesting results can be obtained:

(1) The whole acceleration time of ions is about 10–20 times of the laser-pulse duration. After that, the separating field is close to zero and the acceleration ends.

(2) The electron density and the electric field reach their maximum values at the time $t=t_l$ as expected by our discussion and the gain energy of ions in the process of the isothermal expansion is approximately a quarter of the final energy. Therefore, the adiabatic expansion is also important for the ion acceleration although the electron density and electric field decrease in this process.

(3) The influence of the hot-electron recirculation on the ion acceleration for thin foils is obvious. The maximum ion energy for thin foils is larger than that for thick targets.

With solutions of $N(\tau)$, the time-dependent electric field and the ion velocity at the ion front can be obtained. Therefore, for the target of arbitrary thickness, the maximum energy of proton beams can be achieved if the laser absorption efficiency is known.

III. COMPARISON WITH EXPERIMENTS

In Appendixes A and B, we show the detail of the solution of the nonlinear Eqs. (5) and (7) using the iterative method. In order to obtain a proper initial value of the iterative process, the nonlinear equations of the density for the simplest case $F_{\theta,3\text{D}}=1$ have been derived in Appendix A. The calculation is accomplished by MATLAB and a main input file has been listed in Appendix B.

Figure 2 shows the comparison between the step model [10], the experimental data from Saclay [12] in ultrahigh-contrast region, and our time-dependent two-phase model. As discussed by Huang *et al.* [10], the laser absorption efficiency decreases for target thickness $L\lesssim1$ μm and quite important for the ion acceleration. Here, with reference to [16], for $L\lesssim1$ μm, the laser absorption efficiency is assumed as

$$\eta=80\%\frac{\ln(1+L)}{1+\ln(1+L)}. \tag{8}$$

For $L\gtrsim1$ μm, laser absorption efficiency is about 40% and does not change almost. From Fig. 2, the following results can be concluded:

(1) The results given by the step model are larger than that given by our model and the experimental data. One of the reasons is the neglect of the dilute effect of the density due to the electron recirculation and the opening angle of the

electrons as discussed in Sec. II A. Another reason is that the decrease of laser absorption could not be accounted in the step model. Therefore, the electron density used in the step model is much larger than the actual one for thin foil: $L \lesssim 1$ μm.

(2) For thin foils, our model is well consistent with the experimental data. It is proved that our model is more valuable for ultrathin foil in the ultrahigh-contrast region.

Our time-dependent model is also compared to other experiments, the results are listed in Table I. For example, for $I=1\times10^{20}$ W/cm^2, $\lambda=0.8$ nm, and $t_l=100$ fs, the critical target thickness is about 15 μm according to Mackinnon *et al.* [8], $E_{\max}(L=30\ \mu\text{m})=6.2$ MeV. With the simulation results (Fig. 12 in [11]), the laser absorption stays constant of about $35\% \rightarrow 50\%$ with the target thickness for thick target, $L \gtrsim 1$ μm. The laser absorption changes with target thickness, the contrast ratio between the main pulse and prepulse, and the prepulse duration [2,10] for $L \lesssim 1$ μm. For different target thicknesses, the permeation of laser pulse is different. For different contrast ratio and prepulse duration, the scale length of the preplasma is different, which induces different laser absorption mechanism. Therefore, the laser absorption efficiency, $\eta(L)$, is different and difficult to be assured. Different $\eta(L)$ corresponds to different electron density, n_{e0}. The plasma frequency and acceleration parameters depend on n_{e0}. After all, the changing law of $\eta(L)$ with L for $L \lesssim 1$ μm is quite important for the proton acceleration and still a challenge. Without $\eta(L)$, our model cannot be compared to experiments for $L \lesssim 1$ μm. However, the laser absorption efficiency for the target of arbitrary thickness has been calculated by PIC simulations [11] although there is no analytic result of that.

With the simulation results in Ref. [11], the small target thickness will lead to reduced absorption if the target deconfines rapidly and becomes transparent before the end of the laser pulse, but the characteristic velocity for this is the sound speed, not the speed of light. If the critical thickness for recirculation is L_c, the critical thickness for modified absorption should be much smaller than L_c. Therefore, for thin foils of the thickness, $L \gtrsim 1$ μm, the laser absorption efficiency keeps a constant about approximately 35%–50% with the thickness L. For the target of 3 μm, $\eta \approx 40\%$, and $\theta_{\text{in}}=17°$, the maximum proton energy is 22.6 MeV estimated by our model which is consistent with the experimental data, 22–24 MeV. The time-dependent electron density, the acceleration field, and the ion speed are shown in Fig. 1(b). The hot-electron density increases from 0 and reaches the maximum value 1.5 at the time t_l. Therefore, for $L=3$ μm and $L_c=15$ μm, the hot-electron recirculation does exist and $N(\tau)$ is up to about 1.5 but not 5 as shown by Sentoku *et al.* [9]. After t_l, the electron density decreases quickly to half at about $2.2t_l$. The durations of the hot-electron density and field are $2-5t_l$.

The maximum value of $N(\tau)$ is smaller than or equal to 1 as shown by Fig. 1. Figure 1 shows that: the maximum $N(\tau)$ is about 0.79 which is smaller than 1, therefore there is no hot-electron recirculation phenomena for $L \geq L_c$; as the time goes to infinite, the velocity of protons is finite and the maximum energy is about 1.1 MeV while the experimental data is 1.2 ± 0.3 MeV; the duration of the hot-electron density is about $3.6t_l$. Therefore, the duration of the field at the ion front is about $2t_l$, which is consistent with the simulation result [11].

IV. SCALING LAWS

The laser intensity in our model is assumed to be a constant value in the pulse duration. Under this assumption and for a fixed laser energy, the dependence of maximum ion energy on the laser-pulse duration is easy to be obtained. There is an optimum pulse duration for the target normal sheath acceleration of ions if the laser energy, focus radius, and absorption efficiency sustain constants. It is a conflict of large acceleration gradient and long efficient acceleration time. For long pulse duration, the intensity will be low and the acceleration field will be low. For a high intensity, the efficient acceleration time will be short. Therefore, there is an optimum pulse duration in the ion acceleration.

For different focus radius and target thickness, the dependence of maximum ion energy, $E_{\max,i}$, on pulse duration can be also obtained easily with our model. The results may be different since the plasma density changes with r_L and L as shown by Eqs. (2) and (3). The wavelength will not influence the dependence of $E_{\max,i}$ on pulse duration.

For a series of given pulse duration, the dependence of $E_{\max,i}$ on laser intensity has also been obtained and the scaling law is given by

$$E_{\max,i}=\begin{cases}\exp(a_1)(I_{10^{18}\ \text{W/cm}^2}\lambda^2_{\mu\text{m}})^{b_1}\text{MeV}, & I_{10^{18}\ \text{W/cm}^2}\lambda^2_{\mu\text{m}} \lesssim 6.4\\ \exp(a_2)(I_{10^{18}\ \text{W/cm}^2}\lambda^2_{\mu\text{m}})^{b_2}\text{MeV}, & I_{10^{18}\ \text{W/cm}^2}\lambda^2_{\mu\text{m}} \gtrsim 6.4,\end{cases} \tag{9}$$

where a_1, a_2, b_1, b_2 are all coefficients and shown by Fig. 3.

With Eq. (9) and Fig. 3, two important results can be obtained. First, the scaling law is different from the previous results $I^{1/2}$. The indexes b_1 and b_2 depend on the laser-pulse duration and decrease with pulse duration. It shows that the adiabatic expansion of plasmas is also a very important acceleration process and should not be neglected, although they [2,4] can consist with experiments considering the isother-

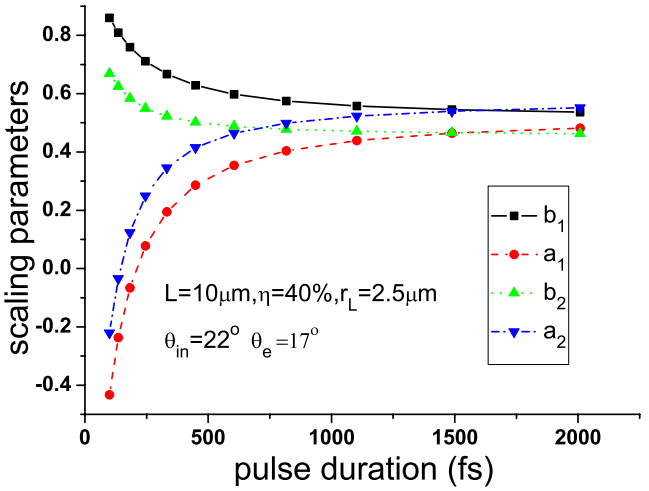

FIG. 3. (Color online) The coefficients in the scaling law given by Eq. (9) versus laser intensity, I. Laser absorption efficiency is assumed 40%, since the target thickness is large enough. Here, focus radius is 2.5 μm.

mal expansion only through adjusting of the parameters η, the acceleration time t_{acc}, the plasma density n_e, the opening angle of electrons, and so on. Second, the influence of hot-electron recirculation on the ion acceleration can be shown by Fig. 3 approximately.

In fact, focus radius influences the electron density and then the ion acceleration. For $L=10$ μm, $\eta=40\%$, $\theta_{\mathrm{in}}=22°$, $\theta_e=17°$, using our model, the effect of focus radius satisfies

$$E_{\mathrm{max},i}=A_2+\frac{A_1-A_2}{1+(r_L/r_0)^p}\mathrm{MeV}, \tag{10}$$

where A_1, A_2, r_0, and p are all coefficients and change with laser intensity, shown in Fig. 4, and r_L is in micrometers. With Eq. (10), some interesting results can be achieved:

(1) The smaller laser intensity, the larger the critical value r_0 and the index p. Therefore, for $r_L \gg r_0$ and $(r_L/r_0)^p \gg 1$, $E_{\mathrm{max},i} \approx -(r_L/r_0)^{-p}$. The derivation of $E_{\mathrm{max},i}$, $dE_{\mathrm{max},i}/d(rL/r_0)=p(r_L/r_0)^{-p-1}$, reflects the rate of change of $E_{\mathrm{max},i}$ to the focus radius. The rate of change is positive but decreases with focus radius. The larger laser intensity, the larger the rate of change.

(2) Oppositely, for $r_L \ll r_0$ and $(r_L/r_0)^p \ll 1$, $E_{\mathrm{max},i} \approx$ constant, which shows that the influence of r_L on the maximum ion energy can be ignored in this case; the larger laser intensity, the smaller critical focus radius. Therefore, the larger laser intensity, the more sensitive the ion acceleration to the change of focus radius.

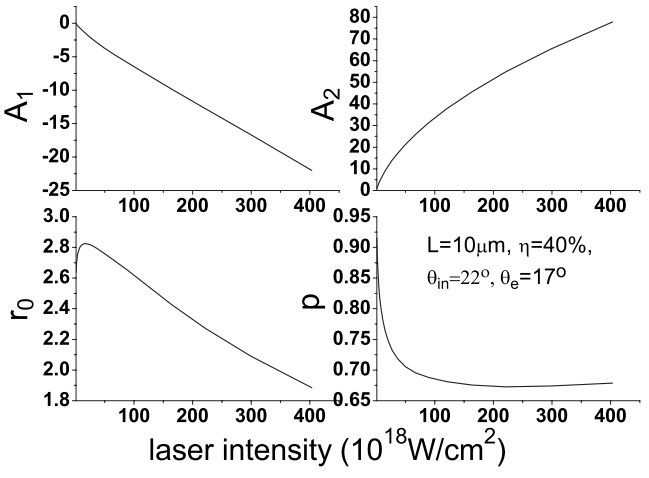

FIG. 4. The coefficients of the scaling law of maximum ion energy with respect to focus radius given by Eq. (10) versus laser intensity for $L=10$ μm, $\eta=40\%$, $t_l=100$ fs, and $\lambda=0.8$ μm.

V. DISCUSSION

The influence of opening angle of hot electrons on maximum ion energy has been discussed in detail by Huang *et al.* [10]. However, the dilution of the electron density as electrons circulate and spread laterally was not contained there. This effect is considered here with the factor, $F_{\theta,3\mathrm{D}}$ in Eqs. (4)–(7). Therefore, the maximum value of $N(\tau)$ here is 1.5 [in Fig. 1(b)] while it is about 5 in Refs. [9,10]. For the target of arbitrary thickness, the maximum energy of ions heated by target normal sheath acceleration (TNSA) can be obtained by this model if the absorption efficiency of laser pulse is given.

Here we will discuss the limits of our model. The prepulse is not considered in our model and the contrast is assumed large about 10^8 which can be achieved in lots of experiments. However, the existence of a prepulse would generate a preplasma and the preplasma size, the scaling length of the preplasma, will most influence the mechanisms of laser absorption and then the temperature of hot electrons. Different laser absorption mechanism results in different generation rate of hot electrons, f, and different hot-electron temperature, T_e. No matter what the mechanisms are, the generation of hot electrons is cumulative and the assumption $f=\bar{f}$ causes little error relative to that caused by the measurement in experiments. Whatever the temperature of hot electrons is, our model is still in use with the actual temperature instead of the value $mc^2(\gamma-1)$. The influence of the prepulse on the laser-plasma heating was investigated by Nuter *et al.* [17] by PIC simulations. However, the analytic theory on the influence of the prepulse on the ion acceleration is still a challenge.

The laser intensity in our model is assumed to be a constant value in the pulse duration. In fact, the intensity is changing with time and the distribution is about Gaussian distribution. However, the actual intensity distribution with respect to time and position when laser pulse is acting on a target is quite difficult to be measured in real time. Since we do not consider the time distribution of laser intensity, we cannot give an estimation of the error. In the next paper, we will consider that case.

VI. CONCLUSION

In conclusion, the time-dependent isothermal expansion and adiabatic expansion for the target normal sheath proton acceleration are discussed. A two-phase model and a scaling law of the maximum energy of proton beams have been proposed. The influence of the hot-electron recirculation on the

ion acceleration has been accounted in. For $L \geq L_c$, the hot-electron recirculation can be ignored. But for $L \leq L_c$, the hot-electron recirculation exists and enhances as the target thickness decreases. The results given by our model have been compared to experiments and shown in Fig. 2 and Table I. The dependence of maximum ion energy on target thickness, focus radius, and laser-pulse duration has been obtained and shown by Eqs. (9) and (10), and Figs. 3 and 4, and so on. At last, the application and limits of our model have been discussed. An interesting work that may be considered next is the time-dependent laser-pulse intensity in order to optimize our model further more.

ACKNOWLEDGMENTS

We acknowledge the support of the Key Project of Chinese National Programs for Fundamental Research (973 Program) under Contract No. 2006CB806004 and the Chinese National Natural Science Foundation under Contract No. 10334110.

APPENDIX A: THE NONLINEAR EQUATION OF THE TIME-DEPENDENT DENSITY FOR $F_{\theta,3D}=1$

In order to solve Eqs. (5) and (7) with the iterative method, we need to find a proper initial value for $N(\tau)$. Fortunately, the solution of the nonlinear equation of the time-dependent density for $F_{\theta,3D}=1$ can be obtained by MATLAB easily and is a proper initial value. In this appendix, we will derive the nonlinear equation of the time-dependent density for $F_{\theta,3D}=1$ in the whole process of the plasma expansion.

The ion acceleration is decided by the electric field. For any time, the maximum electric field is at the ion front and decided by the plasma density and temperature. From the Poisson's equation, it is shown that the field is proportional to the square root of the density. With our beat knowledge, the electric field is also proportional to the square root of the plasma temperature (the electron temperature) [6]. Therefore, with Eq. (6), the ion velocity is given by

$$u(\tau) = 2\int_0^{\tau} \sqrt{\frac{N(\tau)}{1+\tau^2}}\, d\tau \tag{A1}$$

in the isothermal process and

$$u(\tau) = 2\int_0^{\tau} \sqrt{\frac{N(\tau)}{1+\tau^2}\left(\frac{\tau}{\tau_l}\right)^{-\gamma+1/\gamma}}\, d\tau \tag{A2}$$

in the adiabatic process. The ion position $l(\tau)$ can be achieved by the integration of the ion velocity. For $F_{\theta,3D}=1$, combining Eqs. (5), (7), (A1), and (A2), the nonlinear equation for the plasma density $N(\tau)$ is written as

$$Z'' = c_0 Z^{-0.5}\sqrt{\frac{\tau}{1+\tau^2}}, \tag{A3}$$

where $Z=\tau/N(\tau)$, $c_0=2\sqrt{2e}\,\tau_1/\hat{L}$, $Z'(0)=0$, and $Z(0)=\tau_1$ in the isothermal process and

$$Z_1'' = c_1 Z_1^{-0.5}\sqrt{\frac{\tau^{-1+\gamma/\gamma}}{1+\tau^2}}, \quad \tau \geq \tau_l, \tag{A4}$$

where $Z_1=1/N(\tau)$, $c_1=\sqrt{2/e}\,\tau_l^{1/2\gamma-1/2}\tau_L/[\hat{L}+\hat{l}(\tau_L)]$, $Z_1'(\tau_l)=u(\tau_1)\tau_L/\tau_l[\hat{L}+\hat{l}(\tau_L)]$, and $Z_1(\tau_l)=\tau_L[\hat{l}(\tau_1)+\hat{L}]/\tau_l[\hat{L}+\hat{l}(\tau_L)]$ in the adiabatic process.

We solve Eqs. (A3) and (A4) with the solving function ODE113 in MATLAB7.0. The solutions of them are used as the initial value of $N(\tau)$ in the iterative-solving process of Eqs. (5) and (7).

APPENDIX B: A MATLAB INPUT FILE FOR THE SOLUTION OF OUR TIME-DEPENDENT MODEL

With the proper initial value given by the solution of Eqs. (A3) and (A4), the time-dependent plasma density is obtained iteratively using Eqs. (5), (7), (A1), and (A2). Then the maximum ion velocity and energy are also achieved. The calculation process is realized by MATLAB [18].

With the MATLAB files, our time-dependent solutions have been obtained for a serial of target thicknesses defined by LLs in micrometers, the laser intensity $I=5$ in 10^{18} W/cm^2, pulse duration Las=65 in femtoseconds, wavelength lambda=0.8 in micrometers, and focus radius $rL=4$ in micrometers. These parameters are from the experiments of Ceccotti *et al.* [12] and our results are compared to their experimental data as shown by Fig. 2.

The whole iterative process is cut into four parts: $t<t_L$, $t_L \leq t \leq t_l$, $t_l < t \leq t_{up1}=150$, $t_{up1} < t \leq t_{up2}=10000$ for $L \leq L_c$. For $L<L_c$, the separate method is a little different and it is easy to accomplish. However, for $L>L_c$, the results given by our model is smaller than the experimental data shown by Fig. 2 and the model of Fuchs *et al.* [4] is suggested.

[1] S. C. Wilks, A. B. Langdon, T. E. Cowan, M. Roth, M. Singh, S. Hatchett, M. H. Key, D. Pennington, A. MacKinnon, and R. A. Snavely, Phys. Plasmas **8**, 542 (2001); L. O. Silva, M. Marti, J. R. Davies, R. A. Fonseca, C. Ren, F. S. Tsung, and W. B. Mori, Phys. Rev. Lett. **92**, 015002 (2004); H. Schwoerer, S. Pfotenhauer, O. Jackel, K. U. Amthor, B. Liesfeld, W. Ziegler, R. Sauerbrey, K. W. D. Ledingham, and T. Esirkepov, Nature (London) **439**, 445 (2006).

[2] M. Kaluza, J. Schreiber, M. I. K. Santala, G. D. Tsakiris, K. Eidmann, J. Meyer-ter-Vehn, and K. J. Witte, Phys. Rev. Lett. **93**, 045003 (2004).

[3] J. Schreiber, F. Bell, F. Gruner, U. Schramm, M. Geissler, M. Schnurer, S. Ter-Avetisyan, B. M. Hegelich, J. Cobble, E. Brambrink, J. Fuchs, P. Audebert, and D. Habs, Phys. Rev. Lett. **97**, 045005 (2006).

[4] J. Fuchs, P. Antici, E. d'Humières, E. Lefebvre, M. Borghesi, E. Brambrink, C. A. Cecchetti, M. Kaluza, V. Malka, M. Manclossi, S. Meyroneinc, P. Mora, J. Schreiber, T. Toncian, H.

Pépin, and P. Audebert, Nat. Phys. **2**, 48 (2006).
[5] L. Robson, P. T. Simpson, R. J. Clarkei, K. W. D. Ledingham, F. Lindau, O. Lundh, T. McCanny, P. Mora, D. Neely, C.-G. Wahlstrom, M. Zepf, and P. McKenna, Nat. Phys. **3**, 58 (2007).
[6] P. Mora, Phys. Rev. Lett. **90**, 185002 (2003).
[7] P. Mora, Phys. Rev. E **72**, 056401 (2005).
[8] A. J. Mackinnon, Y. Sentoku, P. K. Patel, D. W. Price, S. Hatchett, M. H. Key, C. Andersen, R. Snavely, and R. R. Freeman, Phys. Rev. Lett. **88**, 215006 (2002).
[9] Y. Sentoku, T. E. Cowan, A. Kemp, and H. Ruhl, Phys. Plasmas **10**, 2009 (2003).
[10] Y. S. Huang, X. F. Lan, X. J. Duan, Z. X. Tan, N. Y. Wang, Y. J. Shi, X. Z. Tang, and Y. X. He, Phys. Plasmas **14**, 103106 (2007).
[11] E. d'Humières, E. Lefebvre, L. Gremillet, and V. Malka, Phys. Plasmas **12**, 062704 (2005).
[12] T. Ceccotti, A. Levy, H. Popescu, F. Reau, P. D'Oliveira, P. Monot, J. P. Geindre, E. Lefebvre, and Ph. Martin, Phys. Rev. Lett. **99**, 185002 (2007).
[13] J. J. Santos, F. Amiranoff, S. D. Baton, L. Gremillet, M. Koenig, E. Martinolli, M. Rabec Le Gloahec, C. Rousseaux, D. Batani, A. Bernardinello, G. Greison, and T. Hall, Phys. Rev. Lett. **89**, 025001 (2002).
[14] R. A. Snavely, M. H. Key, S. P. Hatchett, T. E. Cowan, M. Roth, T. W. Phillips, M. A. Stoyer, E. A. Henry, T. C. Sangster, M. S. Singh, S. C. Wilks, A. MacKinnon, A. Offenberger, D. M. Pennington, K. Yasuike, A. B. Langdon, B. F. Lasinski, J. Johnson, M. D. Perry, and E. M. Campbell, Phys. Rev. Lett. **85**, 2945 (2000).
[15] D. S. Dorozhkina and V. E. Semenov, Phys. Rev. Lett. **81**, 2691 (1998); A. V. Baitin and K. M. Kuzanyan, J. Plasma Phys. **59**, 83 (1998); V. F. Kovalev, V. Yu. Bychenkov, and V. T. Tikhonchuk, JETP **95**, 226 (2002); V. F. Kovalev and V. Yu. Bychenkov, Phys. Rev. Lett. **90**, 185004 (2003).
[16] A. Andreev, A. Levy, T. Ceccotti, C. Thaury, K. Platonov, R. A. Loch, and Ph. Martin, Phys. Rev. Lett. **101**, 155002 (2008).
[17] R. Nuter, L. Gremillet, P. Combis, M. Drouin, E. Lefebvre, A. Flacco, and V. Malka, J. Appl. Phys. **104**, 103307 (2008).
[18] See EPAPS Document No. E-PLEEE8-79-113903 for the main MATLAB file and two function files hys1 and hys2 for solution of our time-dependent model for $L < L_c$. For more information on EPAPS, see http://www.aip.org/pubservs/epaps.html.